

Parametric Decay of Lower-Hybrid Waves in the ACT-1 Toroidal Device

King-Lap Wong and Masayuki Ono

Plasma Physics Laboratory, Princeton University, Princeton, New Jersey 08544

(Received 12 January 1981)

Nonresonant parametric decay of lower-hybrid waves, observed in a number of high-power tokamak rf-heating experiments, is positively identified as a decay into ion-cyclotron quasimodes. The decay-wave spectrum, wavelength, and amplitude profile are measured inside a toroidal plasma with pump frequency $f_0 \sim 3.5f_{pi} \sim 25f_{ci}$.

PACS numbers: 52.35.Mw, 52.50.Gj, 52.55.Gb

Lower-hybrid-wave heating of magnetized plasmas is a promising candidate for tokamak ignition because of the readily available microwave power and the desirable features of slow-wave coupling structure and phased-waveguide arrays. However, at the high power levels required for tokamak heating, various nonlinear phenomena can occur. One well-known nonlinear phenomenon is the parametric decay¹⁻⁷ of lower-hybrid waves in which the frequencies of the decay waves are observed to be separated roughly by the ion-cyclotron frequency, f_{ci} . This decay spectrum has become a characteristic of lower-hybrid-wave heating in tokamaks. It has been observed in ATC,⁶ JFT-2,⁷ Doublet-IIA,⁸ WEGA,⁹ PETULA,¹⁰ and Alcator A.¹¹ In all these experiments, the decay frequency spectrum was detected by a probe placed in the limiter shadow but, because of the difficulties in wavelength measurements, the component waves were never identified. Various conjectures were made, based on the observed decay spectrum. The spectrum has been

attributed to nonresonant decay (lower-hybrid wave \rightarrow lower-hybrid wave + ion-cyclotron quasimode) in the ATC experiment,⁶ and to resonant decay (lower-hybrid wave \rightarrow lower-hybrid waves + ion-cyclotron waves) in the JFT-2 experiment.⁷ In this paper, we present positive experimental evidence for the nonresonant decay by measuring the wave number. Unlike previous linear machine experiments,^{12,13} the wave in the present experiment was excited by a slow-wave structure in the frequency range $f_0 \sim 3.5f_{pi} \sim 25f_{ci}$, very similar to the tokamak experiments. Therefore the experiment described here provides a good simulation of the parametric decay process that can occur near the tokamak edge, a process which can be critically important^{4,5} to the heating efficiency. However, the final determination of the amount of pump depletion that may occur in a high-power tokamak heating experiment still awaits further theory and experimentation.

The growth rate of the parametric decay instability can be calculated from¹

$$\gamma = -\Gamma_2 - \frac{\mu^2}{4|\partial/\partial\omega_2[\text{Re}(1+\chi_i^- + \chi_e^-)]|} \text{Re} \frac{i\chi_e\chi_i}{1+\chi_i+\chi_e}, \quad (1)$$

where μ is the parametric coupling coefficient¹; χ_i and χ_e are the ion and electron susceptibilities for the low-frequency decay waves, and the superscript minus sign refers to the lower sideband mode; J_0 and J_1 are the Bessel functions of the first kind; Re denotes the real part of a complex quantity; and ω_2 and Γ_2 are the frequency and the damping rate of the sideband mode. Figure 1 shows the calculated growth rate as a function of the decay wave frequency for our experimental parameters. Collisional damping and electron Landau damping are included in Γ_2 , and the parallel wave number ($k_{||}$) of the decay wave is used as a free parameter to maximize the growth rate. The periodic variation of the growth rate (with

period $\sim f_{ci}$) is due to oscillations in the ion susceptibility as a function of frequency. This behavior will explain the decay spectrum shown in Fig. 2(b). The convective decay threshold can be estimated from¹

$$\gamma > \pi v_2 / L_z, \quad (2)$$

where L_z is the antenna length and v_2 is the parallel phase velocity of the sideband.

The experiment was performed in the Princeton ACT-1 device, which is a steady-state toroidal machine operating at the following parameters: toroidal field $B_0 \leq 5.6$ kG; plasma density $n \sim (1-6) \times 10^{10}$ cm⁻³; electron temperature $T_e \sim 5$ eV;

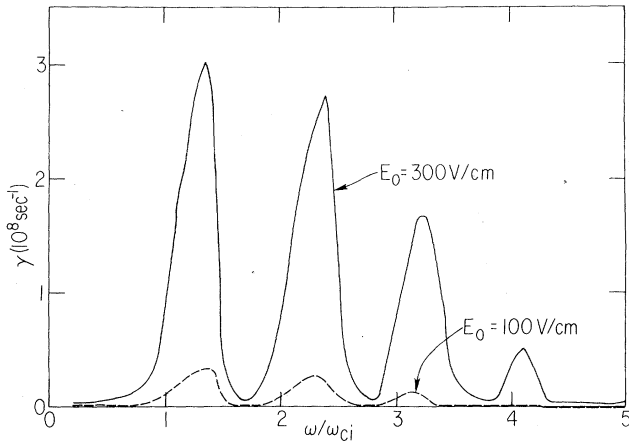


FIG. 1. Variation of growth rate as a function of decay wave frequency at $n = 5 \times 10^{10} \text{ cm}^{-3}$, $B_0 = 3.8 \text{ kG}$, $T_e = 5 \text{ eV}$, $T_i = 1.5 \text{ eV}$ (hydrogen plasma).

ion temperature $T_i \sim 1.5 \text{ eV}$ (determined by test waves near the ion cyclotron frequency)¹⁴; neutral hydrogen pressure $(3-5) \times 10^{-5} \text{ Torr}$ (gauge). The plasma has a minor radius $a \approx 9 \text{ cm}$ and major radius $R = 59 \text{ cm}$. Lower-hybrid waves at 160 MHz are excited by an eight-ring antenna¹⁵ with parallel wavelength $\lambda_{\parallel} \approx 6 \text{ cm}$. Figure 2(a) shows, in schematic fashion, the experimental setup, and a typical parametric decay spectrum is shown in Fig. 2(b). Upon varying the magnetic field, the frequency of the low-frequency oscillations may be seen to increase with the ion-cyclotron frequency, as in Fig. 2(c).

Figure 3 depicts the experimental setup for perpendicular interferometric wavelength measurements. This technique can easily achieve 10% accuracy for waves with well-defined wavelengths. Only four to five fringes are observed in typical interferograms of the first sideband mode indicating that the spread in k_{\perp} can be 20% or more. The parallel wavelength is measured by the phase shift between two probes 5 mm apart situated on the same field line. The probe tips are aligned with the test-wave technique as described in the following: A lower-hybrid test wave with known wavelength ($\lambda_{\parallel} = 5 \text{ cm}$, $\lambda_{\perp} = 3.5 \text{ mm}$) is launched towards the probes with the same frequency (154 MHz) and polarization as the sideband mode. The phase shift between the two probe signals is measured by a vector voltmeter (Hewlett-Packard, model No. HP-8405A) which can measure phase difference between coherent signals accurate to within 1 deg. The probes are aligned so that the phase shift is within 10% of the actual value. The measured sideband wavelength ($\lambda_{\parallel} \approx 3.7$

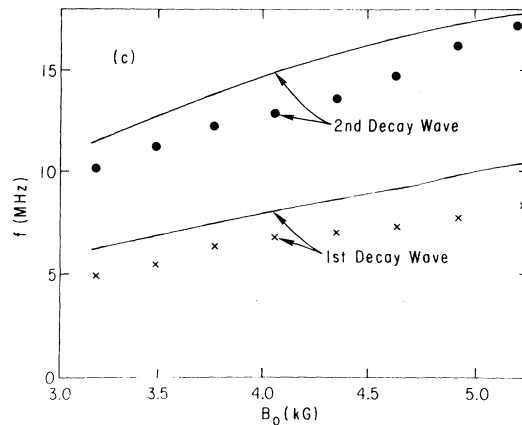
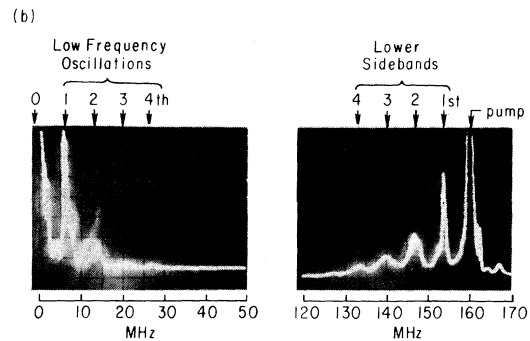
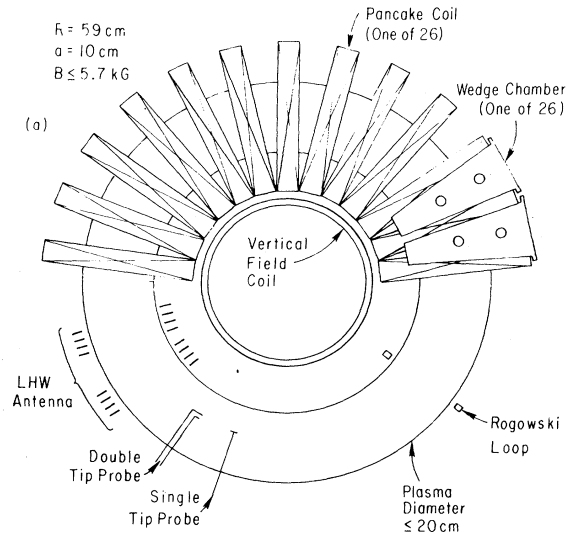


FIG. 2. (a) Schematic of the ACT-1 device. (b) Parametric decay spectrum at $n \sim 5 \times 10^{10} \text{ cm}^{-3}$, $B_0 \approx 3.8 \text{ kG}$, $T_e \sim 5 \text{ eV}$, $T_i \sim 1.5 \text{ eV}$ (hydrogen). (c) Variation of decay wave (low-frequency daughter wave) frequency with magnetic field at plasma center ($r = 0$). The solid line shows the decay wave frequency for which Eq. (2) gives the maximum growth rate.

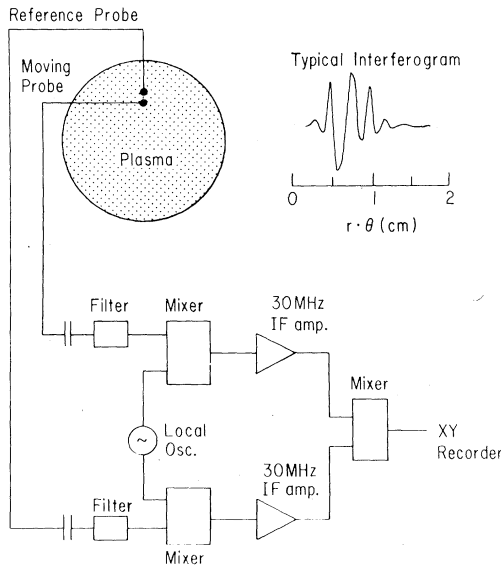


FIG. 3. Schematic of the experimental setup for interferometry measurements.

cm) has a larger uncertainty ($\sim 20\%$) because its wavelength is shorter than the test wave. The first sideband ($\lambda_{\perp} \approx 2.5$ mm, $\lambda_{\parallel} \approx 3.7$ cm) is identified as a lower-hybrid wave that obeys the dispersion relation $\omega \approx \omega_{pe} k_{\parallel} / k_{\perp}$. We have assumed that the sideband parallel wave number has the same sign as the pump wave to get $\lambda_{\parallel} \approx 3.7$ cm. If they have opposite signs, then the sideband has $\lambda_{\parallel} \approx 0.58$ cm, which does not correspond to any normal mode of the plasma; therefore we rule out such a possibility. Waves in the other sidebands are not sufficiently coherent for clean interferograms, indicating that they propagate with a wide range of \vec{k}_{\perp} which washes out the interference fringes. Guided by the measured wavelength and frequency, we calculate $\epsilon(\omega, k)$ for $5 \text{ MHz} \leq \omega/2\pi \leq 7 \text{ MHz}$, $0.2 \text{ cm}^{-1} \leq k_{\parallel} \leq 2.0 \text{ cm}^{-1}$, and find that $|\epsilon(\omega, k)| \gg 1$ everywhere which shows that the low-frequency decay wave must be a forced oscillation (quasimode) that can exist only in the presence of the pump field. This behavior is true as well in tokamaks and can be understood as follows: A weakly damped electrostatic wave must have $\omega/k_{\parallel} \gtrsim 3V_{Te}$ or $\omega/k_{\parallel} \lesssim 0.2V_{Te}$ in order to avoid strong electron Landau damping; such a condition cannot be satisfied with $\omega \sim n\omega_{ci}$ ($n=1-10$) in typical tokamak lower-hybrid-wave experiments where $\omega_0 \sim 25\omega_{ci}$, $\omega_0 \lesssim 5\omega_{pi}$. Therefore resonant decay into electrostatic waves is unlikely to occur under these conditions.

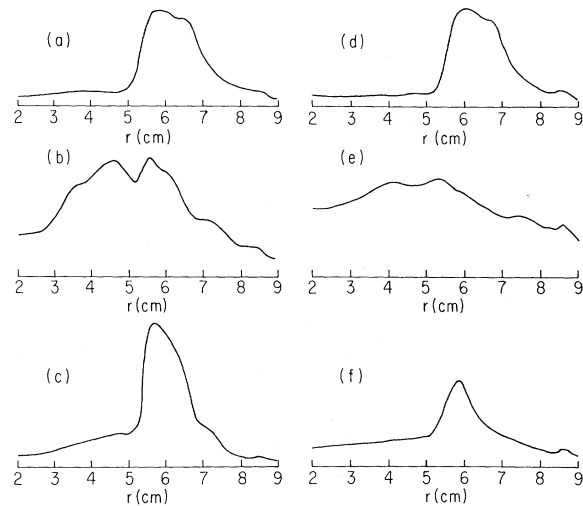


FIG. 4. Radial amplitude profiles of the pump, sideband, and low-frequency decay waves at $B_0 \sim 3.8$ kG, $n \sim 4 \times 10^{10} \text{ cm}^{-3}$. (a) Pump, (b) first sideband, (c) first low-frequency decay wave, (d) pump, (e) second sideband, and (f) second low-frequency decay wave.

Figure 4 shows radial profiles for the pump and decay wave amplitudes. The pump wave is localized along the resonance cone trajectory near the antenna (30 cm from center of antenna) where the measurement was made. In order for the resonant daughter waves to stay inside the pump, they must have $|k_r/k_{\parallel}| = |k_{or}/k_{o\parallel}|$, which is usually not true for $(\vec{E} \times \vec{B})$ -driven decay. The first sideband spreads outside the pump; the second sideband (and also the third and fourth sidebands) propagates all over the plasma, again indicating a wide spread in \vec{k}_{\perp} . Figures 4(b) and 4(e) show that the sideband wave amplitudes tend to get larger at a smaller minor radius apparently because of the focusing effect. It should be noted that the pump wave does not have good poloidal symmetry because of the asymmetric plasma density. Unlike the sidebands, the low-frequency decay waves are localized inside the pump resonance cone. The peaking of their amplitudes is sharper than one would expect from plasma boundary effects. This is because they are not normal modes of the plasma. They are heavily damped outside the pump region and therefore their amplitudes drop abruptly outside the pump resonance cone. From these data, it is obvious that the decay-wave spectrum has a strong spatial dependence. In tokamak experiments, probes can only survive inside the limiter shadow. Conclusions concerning the variation of the parametric

decay instability at various plasma parameters⁷ based on signals from a fixed probe should be treated with caution.

At the operating density $n \approx 5 \times 10^{10} \text{ cm}^{-3}$, the decay threshold is about 25 W net forward power which corresponds to $E_0 \approx 140 \text{ V/cm}$. It is in reasonable agreement with the convective threshold ($E_0 \sim 200 \text{ V/cm}$) calculated from Eq. (2) but much higher than the uniform pump threshold ($E_0 \sim 30 \text{ V/cm}$).

In conclusion, in an experiment on the ACT-1 toroidal plasma, we have identified the parametric decay of the lower-hybrid wave into an ion-cyclotron quasimode. The results, which are in good agreement with theory, are highly pertinent to high-power lower-hybrid heating experiments on tokamaks where the occurrence of such parametric decay at the plasma edge may seriously reduce the rf-heating efficiency.

One of the authors (K.L.W.) would like to thank Professor M. Porkolab, Professor A. Bers, and Professor T. H. Stix for helpful discussions. Technical assistance by Mr. J. Taylor, Mr. W. Kineyko, and Mr. G. Wurden is gratefully appreciated. This work was supported by U. S. Department of Energy Contract No. DE-AC02-76-CH0-3073.

¹M. Porkolab, Phys. Fluids 17, 1432 (1974), and 20, 2058 (1977).

²K. L. Wong, P. Bellan, and M. Porkolab, Phys. Rev. Lett. 40, 554 (1978); K. L. Wong, J. R. Wilson, and M. Porkolab, Phys. Fluids 23, 96 (1980).

³V. K. Tripathi, C. Grebogi, and C. S. Liu, Phys. Fluids 20, 1525 (1977).

⁴L. Chen and R. L. Berger, Nucl. Fusion 17, 779 (1977).

⁵E. Villalon and A. Bers, Nucl. Fusion 20, 243 (1980).

⁶M. Porkolab, S. Bernabei, W. M. Hooke, R. W. Motley, and T. Nagashima, Phys. Rev. Lett. 38, 230 (1977).

⁷T. Imai, T. Nagashima, T. Yamamoto, K. Uehara, S. Konoshima, H. Takeuchi, H. Yoshida, and N. Fujisawa, Phys. Rev. Lett. 43, 586 (1979).

⁸J. Lohr, V. S. Chan, A. F. Lietzke, J. L. Luxon, C. P. Moeller, and D. F. Vaslow, Bull. Am. Phys. Soc. 22, 1163 (1977).

⁹C. Gormezano, P. Blanc, M. Durvaux, W. Hess, G. Ichchenko, P. Lallia, R. Magne, T. K. Nguyen, H. D. Pacher, G. W. Pacher, F. Söldner, G. Tonon, and J. G. Wegrowe, in Proceedings of the Third Topical Conference on Radio Frequency Plasma Heating, California Institute of Technology, Pasadena, 1978 (unpublished), paper A3.

¹⁰P. Briand, L. Dupas, S. N. Golovato, C. M. Singh, G. Melin, P. Grelot, R. Legardeur, and S. Zymanski, in Proceedings of the Seventh International Conference on Plasma Physics and Controlled Nuclear Fusion Research, Innsbruck, Austria, 1978 (International Atomic Energy Agency, Vienna, Austria, 1979), Vol. I, p. 65.

¹¹J. Schuss, private communication.

¹²G. R. Allen, D. K. Owens, S. W. Seiler, M. Yamada, H. Ikezi, and M. Porkolab, Phys. Rev. Lett. 41, 1045 (1978).

¹³M. Ono, M. Porkolab, and R. P. H. Chang, Phys. Fluids 23, 1675 (1980).

¹⁴M. Ono and K. L. Wong, Phys. Rev. Lett. 45, 1105 (1980).

¹⁵K. L. Wong, R. Horton, and M. Ono, Phys. Rev. Lett. 45, 117 (1980).

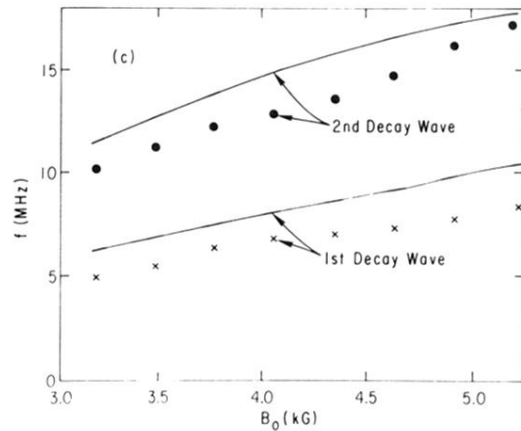
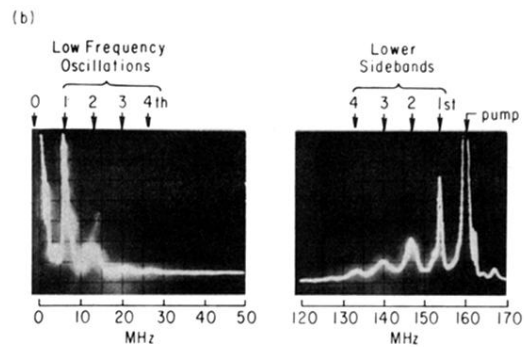
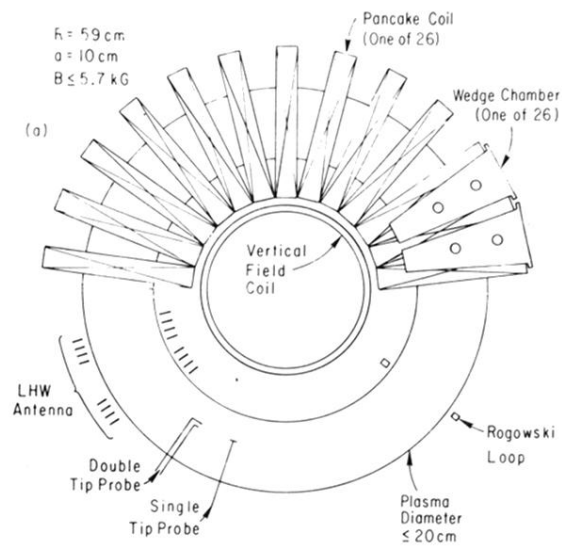


FIG. 2. (a) Schematic of the ACT-1 device. (b) Parametric decay spectrum at $n \sim 5 \times 10^{10} \text{ cm}^{-3}$, $B_0 \approx 3.8 \text{ kG}$, $T_e \sim 5 \text{ eV}$, $T_i \sim 1.5 \text{ eV}$ (hydrogen). (c) Variation of decay wave (low-frequency daughter wave) frequency with magnetic field at plasma center ($r = 0$). The solid line shows the decay wave frequency for which Eq. (2) gives the maximum growth rate.